

Neural Correlates of Animacy Attribution Include Neocerebellum in Healthy Adults

Allison Jack and Kevin A. Pelphrey

Child Study Center, Yale University, New Haven, CT, USA

Address correspondence to Allison Jack, Yale Child Study Center, 230 South Frontage Rd., New Haven, CT 06519, USA.
Email: allison.jack@yale.edu

Recent work suggests that biological motion perception is supported by interactions between posterior superior temporal sulcus (pSTS) and regions of the posterior lobe of the cerebellum. However, insufficient attention has been given to cerebellar contributions to most other social cognitive functions, including ones that rely upon the use of biological motion cues for making mental inferences. Here, using adapted Heider and Simmel stimuli in a passive-viewing paradigm, we present functional magnetic resonance imaging evidence detailing cerebellar contributions to animacy attribution processes in healthy adults. We found robust cerebellar activity associated with viewing animate versus random movement in hemispheric lobule VII bilaterally as well as in vermal and paravermal lobule IX. Stronger activity in left Crus I and lobule VI was associated with a greater tendency to describe the stimuli in social-affective versus motion-related terms. Psychophysiological interaction analysis indicated preferential effective connectivity between right pSTS and left Crus II during the viewing of animate than random stimuli, controlling for individual variance in social attributions. These findings indicate that lobules VI, VII, and IX participate in social functions even when no active response is required. This cerebellar activity may also partially explain individual differences in animacy attribution.

Keywords: cerebellum, connectivity, fMRI, mentalizing, superior temporal sulcus

Introduction

Investigators who focus on understanding the “social brain” have not typically given much consideration to the cerebellum. While a growing body of the literature indicates that activity in topographically distinct regions of the cerebellum is associated with a variety of cognitive and affective functions, particularly in its posterior-lateral hemispheres (the neocerebellum) (Stoodley and Schmahmann 2009, 2010), its potential contribution to specifically social processes has been understudied. However, we might expect it to contribute to social brain function based on current theories about the nature of cerebellar processing and its patterns of connectivity.

The cellular architecture of the cerebellum is remarkably uniform (Eccles et al. 1967; Bloedel 1992), yet the structure participates in a wide array of processes, both motor and cognitive. It has been theorized that the contribution of the cerebellum to this diversity of functions lies in the application of a similar neural operation in the context of differing, highly specific afferent and efferent connections (Bloedel 1992; Ito 1993; Ramnani 2006). The function of this uniform cerebellar operation might be to increase the efficiency of relatively routine cerebral processes, with the cerebral process to which this contribution is made determined by patterns of cerebro-cerebellar connectivity (Schmahmann 1991; Ito 1993; Ramnani 2006). While the anterior lobe (lobules I–V) and lobule VIII of the cerebellum are connected to motor cortex, lobule VII and

portions of lobule VI of the posterior lobe are connected to prefrontal, posterior parietal, and temporal regions (Sasaki et al. 1975; Schmahmann and Pandya 1991; Kelly and Strick 2003; Salmi et al. 2010; Stoodley and Schmahmann 2010; Sokolov et al. 2014). Temporo-cerebellar connectivity may be particularly relevant to social cognition. Temporal lobe, particularly superior temporal sulcus (STS), is critical for social information processing. Its social perceptual functions, especially biological motion processing, are rapid and relatively automatic (Adolphs 2009, 2010). Connectivity from this region to cerebellum via pons has been demonstrated in nonhuman primates (Schmahmann and Pandya 1991). In humans, probabilistic tractography indicates a loop between STS and Crus I, a region of cerebellar posterior lobe (Sokolov et al. 2014). Theoretically, the cerebellum should contribute to the basic social perceptual functions supported by STS, given that these functions are 1) routinized and 2) subserved by a cerebral region with robust cerebellar connectivity.

Initial evidence supports this hypothesis. Lesion work indicates that injury to left posterior-lateral cerebellum disrupts the ability to detect biological motion (Sokolov et al. 2010). Further, independent groups have implicated a region of cerebellar lobule VII, Crus I, as contributing to biological motion perception via interactions with posterior STS (pSTS) (Jack et al. 2011; Sokolov et al. 2012). The finding of cerebellar contributions to biological motion perception, a foundational social cognitive ability (Pavlova 2012), prompted us to consider whether similar effects might be found when investigating a related social ability also known to be partially supported by pSTS activity: animacy attribution.

Previous studies documenting a relationship among Crus I, pSTS, and biological motion perception used stimuli derived from human movements, whether video or point-light stimuli. Animacy attribution paradigms, on the other hand, use the movements of abstract stimuli to suggest that the geometric shapes depicted are animate, and often, that they have emotions, personalities, and social relationships. The degree to which individuals “see” social content in these stimuli varies, and may be deficient in disorders that affect social cognition such as autism (Klin 2000). However, as Heider and Simmel (1944) noted in their seminal study of the phenomenon among healthy adults the overwhelming tendency is to see the shapes as animate creatures, and usually as people. Neuroimaging work on the phenomenon has further expanded our understanding of the neural bases of spontaneous animacy attribution, which typically include fusiform gyrus (FFG), temporal poles (TmP), amygdala (Amy), pSTS, temporo-parietal junction (TPJ), and medial prefrontal cortex (mPFC) (Castelli et al. 2000; Martin and Weisberg 2003; Schultz et al. 2003; Ohnishi et al. 2004; Gobbini et al. 2007; Pavlova et al. 2010; Ross and Olson 2010; Tavares et al. 2011; Jack et al. 2012; Osaka, Ikeda, and Osaka 2012).

While cerebellar activity has been documented in the context of animacy attribution (Ohnishi et al. 2004; Gobbini et al. 2007), its appearance in the literature has been rare relative to the number of studies conducted using variants of the paradigm. Current reporting practices make it difficult to determine whether this low visibility in the literature is due to weak or absent cerebellar effects, or to methodological constraints. It is relatively common to use a functional slice prescription that cuts off the cerebellum, either in whole or in part, in order to capture the cerebrum in greater detail. However, the extent of functional slice prescription is often not described in published reports. When surveying the literature, this can lead to an assumption that the cerebellum is not involved in a particular cognitive process when in fact its role has not been assessed. In the cases in which cerebellar activity related to animacy attribution has been reported, the peak cerebellar activity occurred in either left Crus I (Ohnishi et al. 2004) or a more inferior portion of left lobule VII, Crus II (Gobbini et al. 2007). This suggests that Crus I may be associated with processing more abstract forms of animate movement involved in this paradigm, as well as the more concrete forms of biological motion perception involved in a point-light walker task (Sokolov et al. 2012) or nonmotor aspects of imitation (Jack et al. 2011).

The aims of this study were to evaluate and characterize cerebellar contributions to animacy attribution processes in healthy adults. We predicted that Crus I of neocerebellum would be involved based on previous research linking this region to biological motion processing via pSTS (Jack et al. 2011; Sokolov et al. 2012). We further predicted that posterior vermis might also be active while viewing animate stimuli, given this region's role in emotional processes (Stoodley and Schmahmann 2010), and the fact that healthy adults often attribute emotional content to these stimuli. Further, we hypothesized that these effects might be stronger in individuals who reported seeing more social content in the stimuli, and that these individual differences might be related to patterns of cerebello-temporal connectivity.

Materials and Methods

Participants

Thirty-nine adults participated in the experimental paradigm of interest in this study; of these 39, 5 were excluded because functional slices did not provide full cerebellar coverage. All individuals provided written informed consent and received a small amount of money for participating. Data from 34 adults (7 men) aged 20–34 years ($M = 25.73$; $SD = 3.61$), with normal or corrected-to-normal vision and no history of neurological or psychiatric illness, were included in final analysis. Degree and direction of hand preference were assessed using the Edinburgh Handedness Inventory (EHI), which yields a continuous laterality quotient (LQ) ranging from –100 (indicating a complete leftward preference) to +100 (complete rightward preference). One participant did not complete an EHI, but self-identified as left-handed. The missing data were imputed by taking the average of the LQ values of all other self-identified left-handers in the sample, resulting in an LQ score of –78. Scores on this inventory indicated that 27 members of the sample were right-handed, 4 left-handed, and 3 ambidextrous, with LQ scores ranging from –100 to 100 (median = 88, $M = 66.47$; $SD = 56.98$). The self-reported racial breakdown of the sample was as follows: 67.65% White ($n = 23$), 26.47% Asian ($n = 9$), 2.94% Black ($n = 1$), and 2.94% of mixed origin ($n = 1$). A subset of participants ($n = 28$, 6 men; $M_{age} = 25.62$; $SD_{age} = 3.75$) provided narratives describing what they saw in the videos (see below). The full sample ($n = 34$) was used to

conduct all main effects analyses, and the subsample was used to conduct subsequent analyses exploring associations between spontaneous attribution of animacy and cerebellar activity and connectivity.

Experimental Design

Experimental stimuli were presented in alternating blocks of 16 s each with no interstimulus interval, consisting of 8 unique blocks of the Animate (ANIM) condition interleaved with 8 blocks of the Random (RAND) condition. Each block consisted of a single video clip. Stimuli were adapted from a set developed by Schultz et al. (2003). Order was counterbalanced across participants; of participants in the final full sample, 15 participants viewed a RAND block first and 19 viewed an ANIM block first. All animations featured 3 white geometric shapes (a triangle, a square, and a circle) moving on a black background with the outline of a stationary box in the middle of the screen. ANIM stimuli featured the shapes moving in ways that could be interpreted as goal-directed or social (e.g., chasing each other, fighting, dancing together, hiding in the box). By contrast, during RAND stimuli the shapes moved at the same average speed as during ANIM conditions while bouncing off the edges of the screen, the box, and each other like billiard balls. While the types of movement differed, the overall amount of motion was kept as similar as possible. Participants were told that they would see video clips with some moving shapes, and instructed to stay still and watch the movies. After the task, participants were prompted to provide an open-ended description of the videos they had seen ("What do you remember about the movies where the shapes moved around?").

Imaging

Images were collected at the Yale University Magnetic Resonance Research Center on a Siemens 3T Tim Trio scanner equipped with a 32-channel head-coil. Whole-brain T_1 -weighted anatomical images were acquired using an MPRAGE sequence (repetition time [TR] = 1900 ms; echo time [TE] = 2.96 ms; flip angle = 9°; field of view [FOV] = 256 mm; image matrix 256 mm²; voxel size = 1 mm³; 160 slices; number of excitations = 1). Whole-brain functional images were acquired using a single-shot, gradient-recalled echo planar pulse sequence (TR = 2000 ms; TE = 25 ms; flip angle = 60°; FOV = 220 mm; image matrix = 64 mm²; voxel size = 3.4 × 3.4 × 4 mm; 34 slices) sensitive to blood oxygen level-dependent (BOLD) contrast. Functional slice prescription was oblique, angled to run beneath the base of the cerebellum and temporal lobes. The full cerebellum and temporal lobes were always obtained as well as the vast majority of the cerebrum; for some participants, a very superior portion of the superior frontal, precentral, or postcentral gyrus was lost. The functional sequence consisted of the acquisition of 181 successive brain volumes, the first 5 of which were discarded to allow for magnetic saturation effects, leaving 176 volumes for analysis (Due to experimenter error, only 176 volumes were collected for one participant, leaving 171 volumes for analysis after discarding initial acquisitions. However, this dataset did not exhibit any volumes excessively contaminated by motion, so no further volumes were removed from this dataset.).

Data Analysis

Neuroimaging analysis was conducted using FSL version 5.0.4 (FMRIB's Software Library, www.fmrib.ox.ac.uk/fsl). Except where otherwise stated, all other statistical analysis was conducted with R version 3.0.2 (2013-09-25) (R Core Team 2012).

Analysis of Narratives

Using the method described in Heberlein and Adolphs (2004), transcripts of participant's spontaneous narratives were analyzed using the text analysis software program Linguistic Inquiry and Word Count (version LIWC Lite7) (Pennebaker et al. 2001, 2007), which provided percentages of words in each sample that belonged to 3 categories of interest: affective Processes, a category that draws from a dictionary of 915 words related to positive and negative emotions; Social Processes ("Social"), a category that draws from a dictionary of 455 words related to human interaction and relationship, as well as nonfirst-person-

singular personal pronouns; and a control category, Motion (“Motion”), which draws from 168 words related to motion. We used these categories to calculate an overall Anthropomorphizing Index (AI) (Heberlein and Adolphs 2004) for each participant, using the formula ([Affect + Social]/Motion). We used this index value as a regressor in exploratory individual differences analyses of our neuroimaging data (see below).

fMRI Analysis

fMRI data processing was conducted using FEAT (fMRI Expert Analysis Tool) Version 6.00, part of FSL. Head motion was detected by center of mass measurements implemented using automated scripts developed for quality assurance purposes and packaged with the BXH/XCEDE suite of tools, available through the Bioinformatics Information Research Network. The criterion for exclusion from data analysis was a deviation from the center of mass in any dimension >4 mm; no participant met this criterion. After quality assurance procedures, the following prestatistics processing was applied: motion correction using MCFLIRT (Jenkinson et al. 2002), slice-timing correction using Fourier-space time-series phase-shifting; nonbrain removal using BET (Smith 2002), spatial smoothing using a Gaussian kernel of FWHM 5 mm, grand-mean intensity normalization of the entire 4D dataset by a single multiplicative factor, and highpass temporal filtering (Gaussian-weighted least-squares straight line fitting, with sigma = 50.0 s). Initial registration to the high resolution structural and to the Montreal Neurologic Institute (MNI) Template standard space image was carried out using FLIRT (Jenkinson and Smith 2001; Jenkinson et al. 2002); registration from the structural to standard space was then further refined using FNIRT nonlinear registration (Andersson, Jenkinson, and Smith 2007a; Andersson, Jenkinson, and Smith 2007b).

For each dataset, ICA-based exploratory data analysis was carried out using MELODIC (Beckmann and Smith 2004) to investigate the possible presence of unexpected artifacts. Two trained raters blind to the hypotheses of the study identified ICA components that they judged to be scanner- or movement-related artifacts; interrater agreement was 78.12%. Thereafter, only components that had been independently identified by both raters as noise were removed, producing a filtered and denoised dataset for use in subsequent analyses.

First-level analysis of the functional data was conducted using FEAT, with time-series statistical analysis carried out using FILM with local autocorrelation correction (Woolrich et al. 2001). FSL’s *fsl_motion_outliers* tool was used on nonmotion-corrected functional data to detect timepoints corrupted by large motion using the DVARS metric described in (Power et al. 2012). A confound matrix was generated identifying timepoints for which the root mean squared (RMS) intensity difference from volume N to volume $N+1$ was greater than the 75th percentile plus 1.5 times the interquartile range. This matrix was used to regress out corrupt timepoints at first level. The subject inclusion requirement on this criterion was that no more than 20% of volumes could be identified as motion outliers; however, no subject met this criterion. Standard motion parameters (6 regressors representing translations and rotations in the x , y , and z dimensions) were also included in the first-level model. A summary of data quality measures for the full sample, including motion metrics and signal to fluctuation noise ratio, can be found in Table 1.

Higher-level analysis was carried out at the whole-brain level using FLAME (FMRIB’s Local Analysis of Mixed Effects) (Beckmann et al. 2003; Woolrich et al. 2004; Woolrich 2008) Stages 1 and 2 with automatic outlier detection and deweighting (Woolrich 2008). Z (Gaussianized T/F) statistic images were thresholded using clusters determined

by $Z > 3$ and a (corrected) cluster significance threshold of $P = 0.05$ (Worsley 2001). LQ (de-means) was included as a regressor of no interest to control for laterality effects. The contrast of interest, ANIM > RAND, was assessed. Exploratory analyses added AI (de-means) as a regressor and assessed at a whole-brain level its association with ANIM > RAND ($Z > 2.3$ and $P = 0.05$).

To better understand the potential interplay between pSTS and neocerebellum during this task, we conducted psychophysiological interaction (PPI) analyses (Friston et al. 1997) using the methods described in (O’Reilly et al. 2012), with seeds in several subregions of pSTS. First-level analysis was carried out in FEAT, with time-series statistical analysis carried out using FILM with local autocorrelation correction. Motion outliers and motion parameters were included as nuisance regressors in the first-level model. The psychological regressor of interest (ANIM > RAND) was convolved with a double-gamma hemodynamic response function (HRF) with temporal filtering applied and a temporal derivative added. The seed from which the physiological regressor was extracted was created by thresholding pSTS results from the main ANIM > RAND group-level contrast at $Z > 5.75$ to isolate clusters exhibiting strong pSTS activity. After thresholding, 3 main clusters were apparent: one in left pSTS, and 2 in right pSTS (one more inferior/posterior, and one more superior/anterior). See Supplementary Figure 1. Note that although seed regions were chosen based on the results of the main analysis, circularity concerns do not apply; because the main effect of task is modeled as a regressor in the PPI analysis, the PPI regressor only detects effects over and above main task effects (O’Reilly et al. 2012). These pSTS seed regions were then registered into the functional space of each individual participant and the individual’s mean timecourse was extracted for use as the physiological regressor. The PPI regressor was the interaction term between the psychological and physiological regressors, with the psychological regressor zero-centered about the minimum and maximum values and the physiological regressor de-means. A regressor of no interest (ANIM + RAND) was included to account for shared variance between trial types; it was convolved with a double-gamma HRF with temporal filtering applied and a temporal derivative added. All convolutions were applied prior to forming the interaction term; thereafter no further convolution was applied. Higher-level PPI analysis was carried out using FLAME 1 and 2 with automatic outlier detection and deweighting. Based on our hypotheses, we used an ROI-based approach applying prethreshold masking on the results of our higher-level analyses to investigate potential PPIs in the cerebellum exclusively. For seeds in right pSTS, a mask of the left posterior lobe of the cerebellum was applied which encompassed left lobules VI, Crus I, Crus II, and VIIb; similarly, for the seed in left pSTS, a mask of the right posterior lobe of the cerebellum was applied which encompassed right lobules VI, Crus I, Crus II, and VIIb. These masks were defined using Diedrichsen’s probabilistic cerebellar atlas normalized with FNIRT (Diedrichsen et al. 2009) and thresholded at 25%. Thresholding was applied at $Z > 2.3$ and $P = 0.05$ (corrected). Regressors for the group mean and for AI (de-means) were tested in the same model.

Results

Neural Correlates of ANIM > RAND

Whole-brain analysis of the ANIM > RAND contrast revealed robust activity not only in amygdala and in temporo-occipital and laterofrontal regions of the cerebral cortex, but also in lobule VII of the neocerebellum bilaterally as well as in cerebellar vermis. Activity in cerebrum demonstrated peaks in posterior STS bilaterally, left precentral gyrus, left caudate, right superior frontal gyrus, left temporal pole, and left anterior temporal fusiform. Additional local maxima in cerebrum were observed in insula, inferior frontal gyrus (pars opercularis), amygdala, paracingulate, and orbitofrontal cortex. See Supplementary Table 1 and Supplementary Figure 2.

The observed neocerebellar cluster demonstrated a peak in left VIIb and extended into adjacent lobules left Crus I and II.

Table 1
Data quality summary statistics

	<i>M</i>	SD	Min.	Max.
Avg. RMS movement (absolute)	0.27	0.26	0.08	1.28
Avg. RMS movement (relative)	0.09	0.04	0.04	0.2
Motion outliers (% of total volumes)	3.43	2.56	0	11.36
Signal to fluctuation noise ratio	131.08	22.21	78.2	169.6

RMS, root mean squared.

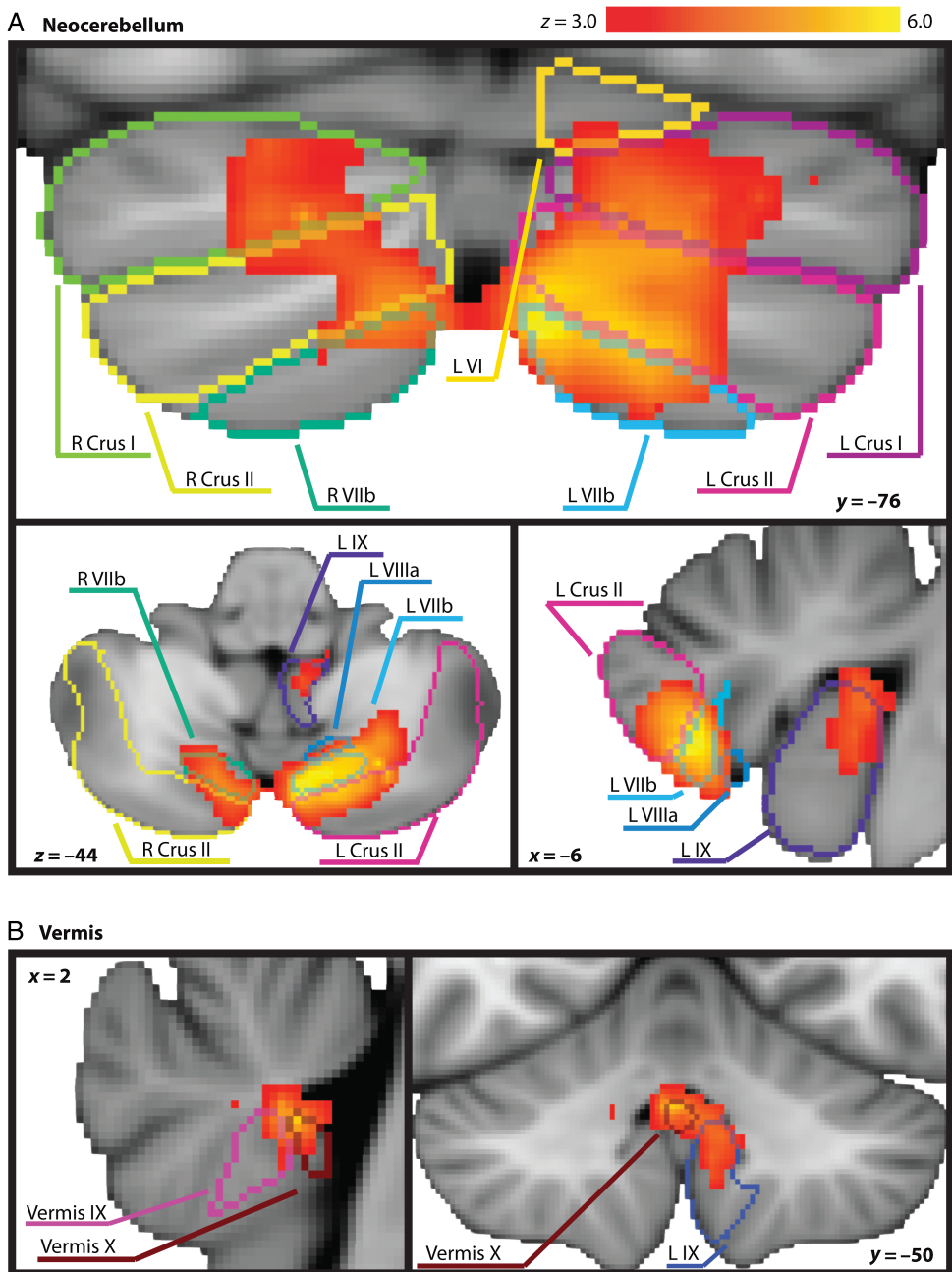


Figure 1. Significant cerebellar activity emerging from the whole-brain Animate > Random contrast is depicted on the MNI standard space template in radiological orientation. Cerebellar lobule outlines from Diedrichsen's probabilistic cerebellar atlas normalized with FNIRT are overlaid on the active clusters as a reference. A (top) highlights neocerebellar clusters, while B (bottom) highlights vermal and paravermal regions.

Activity was observed in the corresponding cerebellar lobules of the right hemisphere, but to a somewhat lesser extent (Fig. 1A). A smaller, more medial cluster also emerged with a peak in Vermis X, which extended into Vermis IX and left lobule IX (Fig. 1B). See Table 2.

Laterality effects were confined to a small cluster in right superior parietal lobule ($x = 30, y = -54, z = 66; Z = 4.70, k = 291$).

Neural Correlates of Individual Differences in Spontaneous Attribution

AIs ranged from -18.18 (more motion references than social-emotional references) to 25 (more social-emotional references

Table 2

Cluster peaks and local maxima of significant cerebellar activity emerging from the whole-brain Animate > Random contrast

Site	Hem	x	y	z	Z	k
VIIb	L	-6	-76	-44	6.42	2913
Crus II	L	-24	-70	-40	5.98	-
VIIa	L	-26	-62	-50	5.87	-
Vermis X	-	2	-50	-32	5.4	264
Vermis IX	-	2	-52	-32	4.93	-
IX	L	-8	-48	-38	4.43	-
X	L	-22	-36	-40	3.76	-
Crus I	R	46	-52	-26	4.28	37

Note: MNI coordinates are reported. Hem, hemisphere; Z: z-statistic; k: voxel extent.

than motion references), with a median of 8.25 ($M = 6.46$, $SD = 11.38$).

Brain response to the ANIM > RAND contrast was significantly associated with AI in both the neocerebellum and in

Table 3
Cluster peaks and local maxima of significant ANIM > RAND activity associated with AI

Site	Hem	x	y	z	Z	k
Crus I	L	-22	-80	-22	4.5	1722
Cerebellar VI	L	-32	-54	-28	3.98	-
Temporo-occipital fusiform	L	-38	-58	-20	3.88	-
Pallidum	R	14	6	0	4.5	952
Putamen	R	24	-2	8	4.09	-
Thalamus	-	-4	-8	10	3.99	-
Superior frontal gyrus	-	-4	56	20	4.05	667
Frontal pole	R	16	56	36	3.88	-
Paracingulate gyrus	-	2	54	16	3.71	-
Posterior STS	L	-44	-84	26	4.61	509

Note: MNI coordinates are reported. Hem: hemisphere; Z: z-statistic; k: voxel extent.

clusters of the pallidum/putamen, dorsomedial prefrontal cortex, and posterior STS (Table 3). The significant cerebellar cluster was characterized by a peak in left Crus I, with local maxima in adjacent left VI, as well as a less robust extension into left Crus II and left VIIb. The mean parameter estimate across this cluster, trimmed to exclude activity extending outside of cerebellum, was $\beta = .78$ ($SD = 0.37$). The positive relationship between AI and ANIM > RAND activity in this cerebellar cluster is depicted in Figure 2.

Cerebello-temporal Connectivity

In our ROI-based PPI analysis interrogating posterior cerebellar regions, we found a significant group mean PPI between the more superior seed in right pSTS and a cluster in the left posterior lobe of the cerebellum with a peak in Crus II ($x = -22$, $y = -76$, $z = -38$; $Z = 3.19$; $k = 226$) and a local maximum in Crus I ($x = -22$, $y = -84$, $z = -30$; $Z = 2.91$). See Figure 2. There were no significant PPI results for the AI regressor.

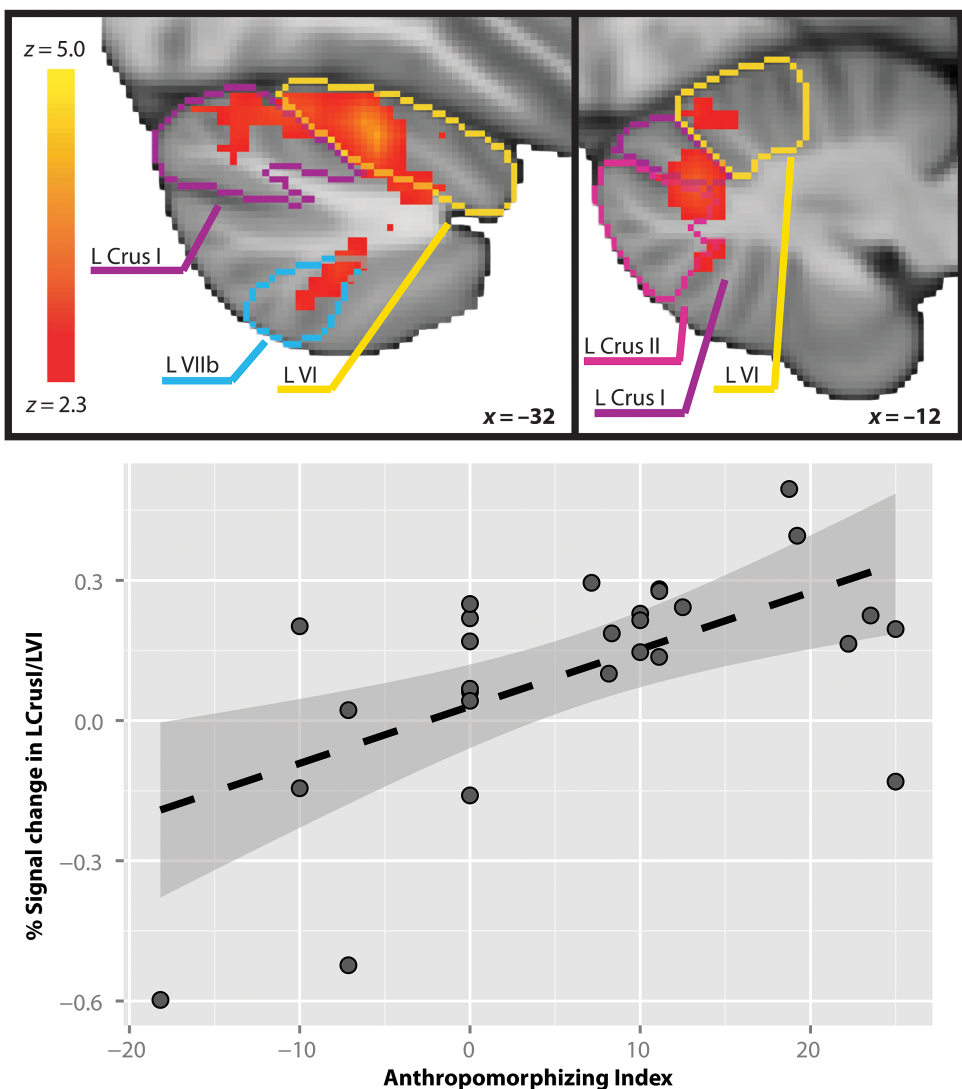


Figure 2. Left Crus I/left VI response to Animate (ANIM) > Random (RAND) is positively related to participants' AI. Top: Cerebellar activity associated with AI is depicted on the MNI standard space template in radiological orientation. Lobule outlines from Diedrichsen's probabilistic cerebellar atlas normalized with FNIRT are overlaid on the active clusters as a reference. Bottom: Percent signal change for the ANIM > RAND contrast extracted from AI-associated brain response in the cerebellar cluster depicted above, with fit line and 95% confidence interval.

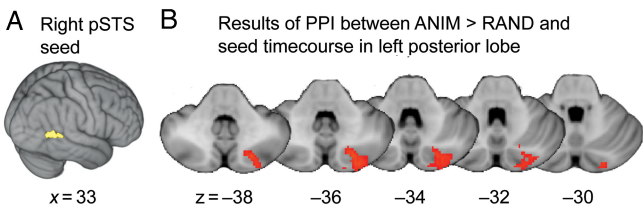


Figure 3. Results of PPI analysis indicating regions of left posterior lobe of the cerebellum whose activity was significantly more strongly correlated with the timecourse of the seed region in right pSTS during Animate than Random trials. (A) Left: The mask of right pSTS from which the average timecourse was extracted to create the physiological regressor. (B) Right: The cluster that emerged from this analysis in left Crus II. Results labeled with MNI coordinates.

PPI analyses using the more inferior right pSTS seed and the left pSTS seed did not yield significant results for either regressor of interest.

Discussion

We found robust cerebellar activity associated with viewing animate versus random movement in VIIb, Crus I, and Crus II bilaterally, and in cerebellar vermis IX–X and left lobule IX. Activity in left Crus I and adjacent left lobule VI was positively associated with participants' AI, or the degree to which they described the stimuli in social-affective versus motion-related terms. Additionally, controlling for individual differences in AI, activity in left Crus II/I was more strongly correlated with activity in right pSTS during the perception of animate than random stimuli.

Neural Correlates of Viewing Animate Stimuli

While the neural correlates of viewing animate stimuli did encompass Crus I as predicted, the strongest activity was in fact more inferior, in VIIb and Crus II. While this activity was somewhat left-lateralized, corresponding right hemispheric activity, particularly in Crus II and VIIb, was apparent as well. This finding was in keeping with Gobbini et al.'s (2007) findings of a Crus II peak related to viewing Heider and Simmel stimuli. In addition, the pattern of activity has parallels in a previous study of biological motion processing in the context of imitation, in which activity not just in bilateral Crus I, but also in left VIIb, was preferentially correlated with right pSTS during imitation of videotaped hand movements versus during equivalent motor movements cued from nonhuman visuospatial signals (Jack et al. 2011). Similarly, engaging in a one-back repetition task using point light displays of biological motion recruits left VIIb as well as left Crus I (Sokolov et al. 2012). In work finding disrupted biological motion detection in patients with left lateral cerebellar lesions, these lesions encompassed lobules VIIb, Crus I, Crus II, and VIIIa (Sokolov et al. 2010). Although there are obvious differences between these paradigms and the current one (active responses versus passive viewing; stimuli derived from human movement versus abstract geometric stimuli), there is overlap in the domain of perceiving animate movement. While these investigations have often focused, particularly when model-testing, on activity in Crus I, it is clear that contributions to biological motion perception (Sokolov et al. 2010, 2012; Jack et al. 2011) and animacy attribution (Gobbini et al. 2007) have been documented in more inferior portions of lobule VII as well. The left-lateralization of these effects is consistent both with the previous research on

biological motion processing specifically, and with the general tendency for spatial processes to elicit peaks in left cerebellar hemisphere (consistent with right-lateralized cerebral control of these processes) (Stoodley and Schmahmann 2009).

The neural correlates of animacy attribution also included posterior vermis, as predicted. These regions included vermal and paravermal lobule IX. While the posterior lateral region of the cerebellum has sometimes been called the “cognitive cerebellum”, the vermis has been called the “limbic cerebellum”, given its connectivity to limbic and paralimbic structures (Schmahmann 2000; Blatt et al. 2013). Posterior vermal activity has been associated with emotional tasks (Stoodley and Schmahmann 2009; Baumann and Mattingley 2012), and acquired lesions or congenital malformations in this area are associated with affective flattening or dysregulation (Schmahmann 1998; Tavano et al. 2007). Vermis IX specifically has been related to anger and disgust induction (Baumann and Mattingley 2012; Schienle and Scharmüller 2013), and viewing negative emotional faces (Schraefel et al. 2012). While viewing the animate stimuli would be expected to involve emotional processing, given that the shapes appear to be interacting in ways driven by emotional states, those states included a mix of positive, affiliative scenarios as well as negative, conflictual scenarios. It is somewhat difficult to reconcile this blend of positive and negative scenarios with vermal lobule IX's apparent bias toward negative emotion. Lobule IX, but not specifically its vermal region, has been identified as contributing to the default mode network (Filippini et al. 2009; Habas et al. 2009). The recruitment of this region in the context of an animacy attribution paradigm may be consistent with the conceptualization of the default mode as in fact a mode of social cognition, which, for typically developing humans, serves as the default state (Schilbach et al. 2008); and with the suggestion that mentalizing activities, in particular, might make up one aspect of default mode processing (Andrews-Hanna, Saxe, and Yarkoni 2014). The activity observed in this paradigm seems to fit best with a social cognitive/mentalizing interpretation.

One possible alternate explanation for the observed pattern of results in lobules VI, VII, and IX could be a preferential response not so much to animacy but rather to unexpected events. Left lobule VI, bilateral lobule VIIb, and left lobule IX have been implicated in detecting changes in stimulus timing, and bilateral lobule V/Crus I and VIIb in detecting change in stimulus orientation (Liu et al. 2008). Animate motion, because driven by internal states and goals, may be inherently less predictable than nonanimate motion that obeys the laws of Newtonian physics. However, during Random motion trials the box in the middle of the screen occasionally opened or closed regardless of contact from the bouncing shapes, and thus was an element of change that could not be predicted either via mentalizing inference or physical inference.

Associations Between Individual Differences in Degree of Animacy Attribution and Cerebellar Activity

The positive relationship between animacy-related activity in left lobule VI/Crus I and individuals' AI scores is compatible with accounts of cerebellar function positing that cerebellar operations on cerebral inputs ultimately support greater routinization and automaticity of the upstream cerebral process (Ramnani 2006). The strongest associations between AI and cerebellar activity were observed in left lobule VI. Meta-analysis indicates that this region tends to be active during spatial tasks and during the

processing of emotional stimuli (Stoodley and Schmahmann 2009). In documenting this pattern, Stoodley and Schmahmann speculated that this extra-verbal activity in emotional paradigms was linked to cognitive or decision-making components of the experimental tasks. Our finding of lobule VI associations with spontaneous social-emotional attributions, however, occurs in the context of a completely passive paradigm: narratives were provided after, not during, the scan. Thus, lobule VI's role is unlikely to be exclusively related to decision-making.

Work on intrinsic connectivity networks has suggested that lobule VI/Crus I participates in the salience (sometimes "limbic salience") network (Habas et al. 2009). This network has prominent dorsal anterior cingulate and frontoinsular nodes, and is thought to be associated with processing stimuli that are personally salient, including emotionally salient stimuli (Seeley et al. 2007). In this case, a graded response in lobule VI/Crus I depending upon how emotionally salient the stimuli were would be compatible with our observed relationship between response in this region and social-emotional attributions.

Cerebello-temporal Connectivity

We identified preferential connectivity between right pSTS and left Crus II/I during the viewing of animate versus random stimuli, controlling for individual differences in the tendency to make social-emotional attributions. Previously, left Crus I has been implicated in humans as potentially forming part of a cerebello-temporal loop with right pSTS, based on both anatomical (Sokolov et al. 2014) and functional (Jack et al. 2011; Sokolov et al. 2012) evidence. Our findings indicate that, while this region does interact preferentially with right pSTS during a task that involves biological motion perception, the strongest contribution to the cerebello-temporal loop in this case comes from left Crus II, complementing our finding of stronger contributions from more inferior portions of lobule VII to the main effects of the ANIM > RAND contrast. The present case differed from paradigms previously used to examine associations between temporal lobe and cerebellum in the context of social cognition, in that it: 1) was passive; 2) was not derived from human movement; and 3) full appreciation of the stimuli required making mental inferences— inferences which drew exclusively upon movement cues. Further work will be necessary to provide a more detailed topographic map of how patterns of cerebello-temporal connectivity vary as a function of task demands. In particular, parametric variation of the level of abstraction of the stimuli, and the nature and degree of the inference required, may help to clarify these patterns.

Conclusion

Overall, these findings indicate that the cerebellum, particularly lobules VI, VII, and IX, participates in social functions, even when no active response is required. Thus, these regions should be considered part of the extended social brain. More generally, this expanding view of the cerebellum suggests the need to be increasingly thoughtful regarding our selection and reporting of imaging protocols. The fact that peaks were elicited in VIIb and lobule IX may partially explain the cerebellum's invisibility in previous instantiations of this paradigm, given that these regions are among the most inferior of the cerebellum, and are frequently cut off in functional slice acquisition, even when the rest of the cerebellum is preserved.

Consequently, these sites are not well understood. Future work should focus specifically on developing our knowledge of these critical regions at the bottom of the brain.

Supplementary Material

Supplementary material can be found at: <http://www.cercor.oxfordjournals.org/>

Funding

This work was supported by the National Institute of Mental Health at the National Institutes of Health (5-T32-MH018268 to trainee A.J.) and Yale University School of Medicine Harris Professorship funds to K.A.P. Neuroimaging analyses were conducted through the Yale Biomedical High Performance Computing Center, using computing clusters made possible by support from the National Center for Research Resources at the National Institutes of Health (S10-RR019895 and S10-RR029676-01).

Notes

The authors would like to acknowledge the valuable assistance of Cara Cordeaux, Suzanna Mitchell, Eva Krapohl, Alex Ahmed, Devon Oosting, Cara Keifer, Hannah Friedman, Charlotte Pretzsch, Danielle Z. Bolling, Diana Mercier, Erin MacDonnell, Heidi Tsapelas, and Daniel Yang, PhD, in recruitment and data collection, with special thanks to C.P., D.Z.B., and H.F. for contributions to data preprocessing, and to Nicole McDonald, PhD, for comments on the final manuscript. We also thank Nicholas J. Carriero, PhD and Robert D. Bjornson, PhD for their assistance with accessing the resources available at the Yale Biomedical High Performance Computing Center. Finally, we would like to express our gratitude to all participants involved in the study.

Conflict of Interest: None declared.

References

- Adolphs R. 2009. The social brain: neural basis of social knowledge. *Annu Rev Psychol.* 60:693–716.
- Adolphs R. 2010. Conceptual challenges and directions for social neuroscience. *Neuron.* 65:752–767.
- Andersson JLR, Jenkinson M, Smith SM. 2007a. Non-linear registration, aka spatial normalisation. Oxford: FMRIB Analysis Group. Report No.: TR07JA2. Available at: www.fmrib.ox.ac.uk/analysis/techrep/2007/02.html.
- Andersson JLR, Jenkinson M, Smith SM. 2007b. Non-linear optimisation. Oxford: FMRIB Analysis Group. Report No.: TR07JA1. Available at: www.fmrib.ox.ac.uk/analysis/techrep/2007/01.html.
- Andrews-Hanna JR, Saxe R, Yarkoni T. 2014. Contributions of episodic retrieval and mentalizing to autobiographical thought: evidence from functional neuroimaging, resting-state connectivity, and fMRI meta-analyses. *Neuroimage.* 91:324–335.
- Baumann O, Mattingley JB. 2012. Functional topography of primary emotion processing in the human cerebellum. *Neuroimage.* 61:805–811.
- Beckmann CF, Jenkinson M, Smith SM. 2003. General multilevel linear modeling for group analysis in fMRI. *Neuroimage.* 20:1052–1063.
- Beckmann CF, Smith SM. 2004. Probabilistic independent component analysis for functional magnetic resonance imaging. *IEEE Trans Med Imaging.* 23:137–152.
- Blatt GJ, Oblak AL, Schmahmann JD. 2013. Cerebellar connections with limbic circuits: Anatomy and functional implications. In: Manto M, Schmahmann JD, Rossi F, Gruol DL, Koibuchi N, editors. *Handbook of the cerebellum and cerebellar disorders.* Dordrecht: Springer Netherlands. p. 479–496.
- Bloedel JR. 1992. Functional heterogeneity with structural homogeneity: how does the cerebellum operate? *Behav Brain Sci.* 15:666–678.
- Castelli F, Happé FG, Frith U, Frith CD. 2000. Movement and mind: a functional imaging study of perception and interpretation of complex intentional movement patterns. *Neuroimage.* 12:314–325.

- Diedrichsen J, Balsters JH, Flavell J, Cussans E, Ramnani N. 2009. A probabilistic MR atlas of the human cerebellum. *Neuroimage*. 46:39–46.
- Eccles JC, Ito M, Szentagothai J. 1967. The cerebellum as a neuronal machine. Berlin, Heidelberg: Springer Berlin Heidelberg.
- Filippini N, MacIntosh BJ, Hough MG, Goodwin GM, Frisoni GB, Smith SM, Matthews PM, Beckmann CF, Mackay CE. 2009. Distinct patterns of brain activity in young carriers of the APOE-epsilon4 allele. *Proc Natl Acad Sci U S A*. 106:7209–7214.
- Friston KJ, Buechel C, Fink GR, Morris J, Rolls E, Dolan RJ. 1997. Psychophysiological and modulatory interactions in neuroimaging. *Neuroimage*. 6:218–229.
- Gobbini MI, Koralek AC, Bryan RE, Montgomery KJ, Haxby JV. 2007. Two takes on the social brain: a comparison of theory of mind tasks. *J Cogn Neurosci*. 19:1803–1814.
- Habas C, Kamdar N, Nguyen D, Prater K, Beckmann CF, Menon V, Greicius MD. 2009. Distinct cerebellar contributions to intrinsic connectivity networks. *J Neurosci*. 29:8586–8594.
- Heberlein AS, Adolphs R. 2004. Impaired spontaneous anthropomorphizing despite intact perception and social knowledge. *Proc Natl Acad Sci USA*. 101:7487–7491.
- Heider F, Simmel M. 1944. An experimental study of apparent behavior. *Am J Psychiatry*. 57:243–259.
- Ito M. 1993. Movement and thought: identical control mechanisms by the cerebellum. *Trends Neurosci*. 16:444–447.
- Jack A, Connelly JJ, Morris JP. 2012. DNA methylation of the oxytocin receptor gene predicts neural response to ambiguous social stimuli. *Front Hum Neurosci*. 6:280.
- Jack A, Englander ZA, Morris JP. 2011. Subcortical contributions to effective connectivity in brain networks supporting imitation. *Neuropsychologia*. 49:3689–3698.
- Jenkinson M, Bannister PR, Brady JM, Smith SM. 2002. Improved optimization for the robust and accurate linear registration and motion correction of brain images. *Neuroimage*. 17:825–841.
- Jenkinson M, Smith SM. 2001. A global optimisation method for robust affine registration of brain images. *Med Image Anal*. 5:143–156.
- Kelly RM, Strick PL. 2003. Cerebellar loops with motor cortex and prefrontal cortex of a nonhuman primate. *J Neurosci*. 23:8432–8444.
- Klin A. 2000. Attributing social meaning to ambiguous visual stimuli in higher-functioning autism and Asperger syndrome: the social attribution task. *J Child Psychol Psychiatry*. 41:831–846.
- Liu T, Xu D, Ashe J, Bushara K. 2008. Specificity of inferior olive response to stimulus timing. *J Neurophysiol*. 100:1557–1561.
- Martin A, Weisberg J. 2003. Neural foundations for understanding social and mechanical concepts. *Cogn Neuropsychol*. 20:575–587.
- Ohnishi T, Moriguchi Y, Matsuda H, Mori T, Hirakata M, Imabayashi E, Hirao K, Nemoto K, Kaga M, Inagaki M et al. 2004. The neural network for the mirror system and mentalizing in normally developed children: an fMRI study. *Neuroreport*. 15:1483–1487.
- O'Reilly JX, Woolrich MW, Behrens TEJ, Smith SM, Johansen-Berg H. 2012. Tools of the trade: psychophysiological interactions and functional connectivity. *Soc Cogn Affect Neurosci*. 7:604–609.
- Osaka N, Ikeda T, Osaka M. 2012. Effect of intentional bias on agency attribution of animated motion: an event-related fMRI study. Greenlee MW, editor. *PLoS One*. 7:e49053.
- Pavlova MA. 2012. Biological motion processing as a hallmark of social cognition. *Cereb Cortex*. 22:981–995.
- Pavlova M, Guerreschi M, Lutzenberger W, Krägeloh-Mann I. 2010. Social interaction revealed by motion: dynamics of neuromagnetic gamma activity. *Cereb Cortex*. 20:2361–2367.
- Pennebaker JW, Chung CK, Ireland M, Gonzalez A, Booth RJ. 2007. The development and psychometric properties of LIWC2007. [Software manual]. Austin, TX: LIWC.net.
- Pennebaker JW, Francis ME, Booth RJ. 2001. Linguistic Inquiry and Word Count: LIWC2001. Mahwah, NJ: Erlbaum Publishers.
- Power JD, Barnes KA, Snyder AZ, Schlaggar BL, Petersen SE. 2012. Spurious but systematic correlations in functional connectivity MRI networks arise from subject motion. *Neuroimage*. 59:2142–2154.
- R Core Team. 2012. R: A Language and Environment for Statistical Computing.
- Ramnani N. 2006. The primate cortico-cerebellar system: anatomy and function. *Nat Rev Neurosci*. 7:511–522.
- Ross LA, Olson IR. 2010. Social cognition and the anterior temporal lobes. *Neuroimage*. 49:3452–3462.
- Salmi J, Pallesen KJ, Neuvonen T, Brattico E, Korvenoja A, Salonen O, Carlson S. 2010. Cognitive and motor loops of the human cerebrocerebellar system. *J Cogn Neurosci*. 22:2663–2676.
- Sasaki K, Oka H, Matsuda Y, Shimono T, Mizuno N. 1975. Electrophysiological studies of the projections from the parietal association area to the cerebellar cortex. *Exp Brain Res*. 23:91–102.
- Schienele A, Schrammüller W. 2013. Cerebellar activity and connectivity during the experience of disgust and happiness. *Neuroscience*. 246:375–381.
- Schilbach L, Eickhoff SB, Rotarska-Jagiela A, Fink GR, Vogeley K. 2008. Minds at rest? Social cognition as the default mode of cognizing and its putative relationship to the 'default system' of the brain. *Conscious Cogn*. 17:457–467.
- Schmahmann JD. 1991. An emerging concept. The cerebellar contribution to higher function. *Arch Neurol*. 48:1178–1187.
- Schmahmann JD. 1998. The cerebellar cognitive affective syndrome. *Brain*. 121:561–579.
- Schmahmann JD. 2000. The role of the cerebellum in affect and psychosis. *J Neurolinguistics*. 13:189–214.
- Schmahmann JD, Pandya DN. 1991. Projections to the basis pontis from the superior temporal sulcus and superior temporal region in the rhesus monkey. *J Comp Neurol*. 308:224–248.
- Schraa-Tam CKL, Rietdijk WJR, Verbeke WJMI, Dietvorst RC, van den Berg WE, Bagozzi RP, De Zeeuw CI. 2012. fMRI activities in the emotional cerebellum: a preference for negative stimuli and goal-directed behavior. *Cerebellum*. 11:233–245.
- Schultz RT, Grelotti DJ, Klin A, Kleinman J, Van der Gaag C, Margis R, Skudlarski P. 2003. The role of the fusiform face area in social cognition: implications for the pathobiology of autism. *Philos Trans R Soc Lond B, Biol Sci*. 358:415–427.
- Seeley WW, Menon V, Schatzberg AF, Keller J, Glover GH, Kenner H, Reiss AL, Greicius MD. 2007. Dissociable intrinsic connectivity networks for salience processing and executive control. *J Neurosci*. 27:2349–2356.
- Smith SM. 2002. Fast robust automated brain extraction. *Hum Brain Mapp*. 17:143–155.
- Sokolov AA, Erb M, Gharabaghi A, Grodd W, Tatagiba MS, Pavlova MA. 2012. Biological motion processing: the left cerebellum communicates with the right superior temporal sulcus. *Neuroimage*. 59:2824–2830.
- Sokolov AA, Erb M, Grodd W, Pavlova MA. 2014. Structural loop between the cerebellum and the superior temporal sulcus: evidence from diffusion tensor imaging. *Cereb Cortex*. 24:626–632.
- Sokolov AA, Gharabaghi A, Tatagiba MS, Pavlova M. 2010. Cerebellar engagement in an action observation network. *Cereb Cortex*. 20:486–491.
- Stoodley CJ, Schmahmann JD. 2009. Functional topography in the human cerebellum: a meta-analysis of neuroimaging studies. *Neuroimage*. 44:489–501.
- Stoodley CJ, Schmahmann JD. 2010. Evidence for topographic organization in the cerebellum of motor control versus cognitive and affective processing. *Cortex*. 46:831–844.
- Tavano A, Grasso R, Gagliardi C, Triulzi F, Bresolin N, Fabbro F, Boratti R. 2007. Disorders of cognitive and affective development in cerebellar malformations. *Brain*. 130:2646–2660.
- Tavares P, Barnard PJ, Lawrence AD. 2011. Emotional complexity and the neural representation of emotion in motion. *Soc Cogn Affect Neurosci*. 6:98–108.
- Woolrich MW. 2008. Robust group analysis using outlier inference. *Neuroimage*. 41:286–301.
- Woolrich MW, Behrens TEJ, Beckmann CF, Jenkinson M, Smith SM. 2004. Multilevel linear modelling for fMRI group analysis using Bayesian inference. *Neuroimage*. 21:1732–1747.
- Woolrich MW, Ripley BD, Brady JM, Smith SM. 2001. Temporal autocorrelation in univariate linear modeling of fMRI data. *Neuroimage*. 14:1370–1386.
- Worsley KJ. 2001. Statistical analysis of activation images. In: Jezzard P, Matthews PM, Smith SM, editors. *Functional MRI: An introduction to methods*. New York: Oxford University Press. p. 251–270.